IIETA International Information and Engineering Technology Association
Advancing the World of Information and Engineering

Revue des Composites et des Matériaux Avancés-Journal of Composite and Advanced Materials
Vol. 35, No. 5, October, 2025, pp. 837-847
Journal homepage: http://iieta.org/journals/rcma

The Role of Coarse Iraqi Bauxite in Tailoring the Microstructure, Physical, and Thermal Properties of Flint-Based Refractory Bricks

Zainab K. Hassan*, Enas M. Hadi, Huda J. Abdulhussein

University of Technology, College of Applied Science, Baghdad 10001, Iraq

Corresponding Author Email: as.23.36@grad.uotechnology.edu.iq

https://doi.org/10.18280/rcma.350504

Received: 8 September 2025
Revised: 9 October 2025
Accepted: 26 October 2025
Available online: 31 October 2025

Keywords:
Iraqi flint-based refractory, coarse grained bauxite aggregate, mullite phase, corundum phase

ABSTRACT

Flint-based refractories are abundant in Iraq but exhibit high shrinkage and poor thermal stability because of their dominant glassy silica phase. Enhancing their performance is essential for producing efficient local materials for high-temperature furnace linings. This study explores the effect of coarse Iraqi bauxite (≤ 1.18mm) as a reinforcing fraction on the microstructure and properties of flint-based refractory bricks. Mixtures containing 10% kaolin and 10-40% coarse bauxite, shaped by uniaxial pressing and sintered at 1350℃ to evaluate phase evolution, densification, and thermal behavior. The pure flint–kaolin sample (A) showed the highest porosity (26%), lowest bulk density (2.08 g/cm³), and largest linear shrinkage (3.8%), governed by the dominant glassy phase. Adding 10% bauxite for (B) reduced porosity to 17.2%, increased density to 2.25g/cm³, and lowered shrinkage to 2.4%. The 20% bauxite sample (C) achieved the best densification with only 8% porosity, 2.32g/cm³ density, and minimal shrinkage (1.9%), attributed to the formation of fine, interlocked mullite. At 30% and 40% bauxite (D, E), porosity rose again (16-18%) due to coarse, loosely packed mullite and corundum, but shrinkage remained low (2.1-2.3%) and density increased to 2.52-3.0 g/cm^3. Thermal conductivity improved progressively from 1.75 W/m·K at 10% to 3.61 W/m·K at 30% for (D), then declined to 0.81 W/m·K at 40% for (E) because of increased pore volume. Overall, coarse Iraqi bauxite effectively controlled shrinkage, promoted loosely packed mullite, and optimized the structural–thermal balance of flint-based refractories.

1. INTRODUCTION

Refractory materials are vital for the stability and efficiency of furnaces and thermal units that operate under severe conditions. Among them, silica-based refractories are widely used due to their high melting point, chemical inertness, and resistance to slag corrosion [1]. However, their intrinsic brittleness, high thermal expansion, and tendency for volumetric shrinkage at elevated temperatures often restrict their service life. In Iraq, flint deposits from the Husseiniyat region have drawn attention as an accessible siliceous raw material for producing refractories, yet their performance remains limited by the high glassy silica content that promotes shrinkage and microcracking during firing [2].

Previous studies have attempted to enhance silica and flint-based refractories through various additives. International works incorporated fine alumina, zirconia, or waste glass to improve sintering and mullite crystallization, achieving denser microstructures but often reducing thermal shock resistance. Hadi [3] mainly focused on refining the fine fraction of flint or mixing it with kaolin and alumina sources to form mullite; however, they primarily used fine powders (< 75 μm), leading to compact but brittle bodies. Sadik et al. [4] presented a detailed review of silica–alumina refractories, outlining how silica-rich sources such as flint and quartz, though chemically stable, suffer from high shrinkage and poor thermal shock resistance at elevated temperatures. They concluded that adding alumina-bearing materials like bauxite or calcined alumina promotes mullite and corundum formation, reduces the glassy phase, and improves dimensional stability. The study emphasized that controlling the SiO_2/Al_2O_3 ratio and particle size distribution is essential for achieving stronger, thermally stable refractories. These insights provided a basis for later works seeking to optimize flint-based refractories through Alumina additions. H. Al-Taie et al. [5] investigated the production and characterization of semi-silica refractory bricks using locally available Iraqi raw materials. Their work focused on combining natural silica sand with kaolin clay to develop cost-effective refractories suitable for furnace linings. The study examined how varying firing temperatures affected phase composition, porosity, bulk density, and thermal stability. Results showed that increasing temperature enhanced sintering, reduced open porosity, and promoted the formation of cristobalite and a limited amount of mullite, improving the mechanical and thermal resistance of the bricks. The authors concluded that Iraqi silica-kaolin compositions could serve as viable raw materials for producing semi-silica refractories with acceptable performance for industrial

applications. The role of coarse particles has been largely overlooked, although coarser aggregates can alter the packing geometry, pore distribution, and crack propagation pathways, thus influencing both shrinkage and thermal stability.

The present work addresses this overlooked aspect by employing coarse Iraqi bauxite fractions (≤ 1.18 mm)—a rich alumina source—added at 10-40 wt% alongside 10 wt% kaolin. This approach diverges from previous fine-scale strategies by intentionally introducing a coarse alumina component to tailor the phase assemblage and microstructural texture. The main objective is to promote the formation of loosely packed, interlocked mullite that balances density, porosity, and shrinkage, thereby improving both thermal and mechanical performance. Through this design, the study establishes a new pathway for optimizing locally developed flint-based refractories and advancing the utilization of Iraqi raw materials in high-temperature industries.

2. EXPERIMENTAL PROCEDURE

Flint and bauxite rocks were obtained from the Husseiniyat area in the Hit district of Anbar Governorate, located along the Euphrates River, approximately 180 km west of Baghdad. The white kaolin clay was collected from the Al-Duwaikhla region in the western desert of Anbar. All raw materials were initially crushed manually, followed by secondary crushing using a jaw crusher. The crushed powders were sieved with an electric vibrator to obtain particle sizes suitable for refractory production, as listed in Table 1.

Table 1. Particles gradient for flint-coarse bauxite-kaolin

Particles Sizes for Ores	
Coarse bauxite	(2.36 ≤ 1.18 mm)
Medium flint	1 - 0.6 mm
Fine flint	0.6 mm
White kaolin	≤ 0.75 mm

The flint ore was pre-fired at 1200℃ to produce burnt flint grog, while bauxite ore was calcined at 1400℃. Both flint and bauxite were chemically analyzed before and after calcination to determine their oxide compositions, as shown in Figures 1-2 and Table 2. Table 2 for refractory batches. Where the refractory mixtures were prepared using flint as the base material, coarse bauxite (≤ 1.18 mm) at different weight ratios of 10-40%, and a fixed 10% addition of fine kaolin (< 0.75 mm), as shown in Table 3. Distilled water (10% by weight) served as the liquid binder.

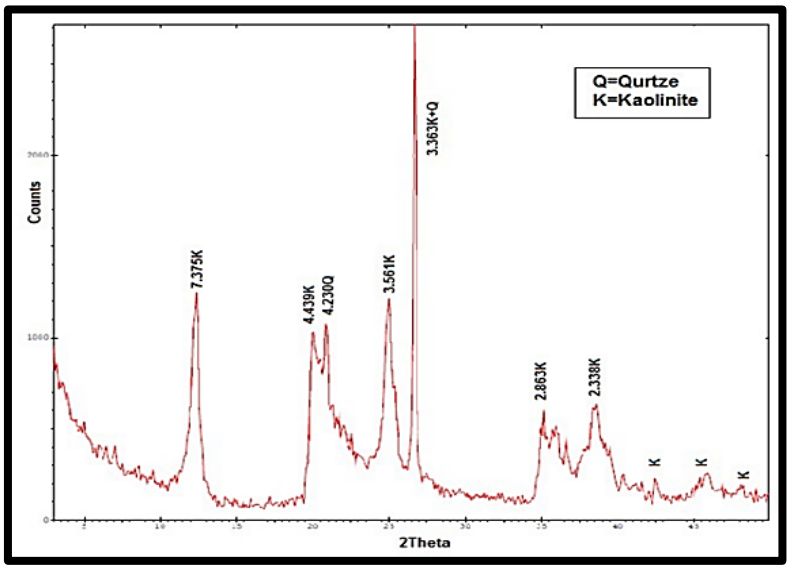

Figure 1. Flint after calcition1200℃ [3]

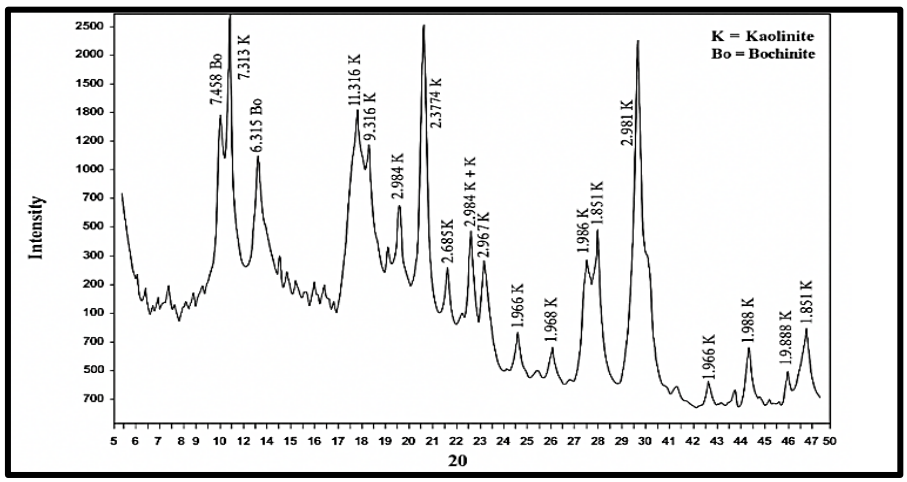

Figure 2. Bauxite raw at 1400℃

Table 2. Chemical analysis for raw materials used in research (where L.O.I. is loss of ignition for raw materials after burning)

Oxides	Kaolin Raw %	Flint Calcined %	Flint Raw %
SiO_2	49.38	40.05	42.05
Al_2O_3	32.72	52.91	38.70
Fe_2O_3	2.07	1.10	0.88
T_iO_2	1.08	2.65	2.20
C_aO	1.19	0.05	1.50
M_gO	0.18	0.01	1.0
$N_{a2}O$	0.22	0.02	0.1
k_2O	0.44	0.02	0.10
SO_3	0.05	0.02	0.03
$L.O.I$	12.3	1.5	11.90

Table 3. Mixtures and their percentages of flint-coarse bauxite-10% kaolin

Batches	(E)	(D)	(C)	(B)	Pure(A)
Coarse bauxite	40%	30%	20%	10%	-
Medium flint	20%	10%	20%	30%	40%
Fine flint	30%	50%	50%	50%	50%
White Kaolin	10%	10%	10%	10%	10%

Cylindrical specimens (5 cm × 1 cm) were formed by uniaxial pressing in hardened steel molds lubricated with paraffin oil. A hydraulic press applying a load of 3 tons was used to ensure uniform compaction. The pressed samples were air-dried at room temperature for 24h, then oven-dried at 110℃ for 6h. Final firing was performed in an electric furnace at 1350℃, following a controlled three-day heating schedule. After sintering, the furnace was switched off and allowed to cool naturally to room temperature overnight till to next day to avoid thermal shock, as shown in Table 4.

Table 4. Firing program (the fourth stage is for the cooling stage)

Stage	Firing Average ℃/min.	Temperature ℃	Soaking Time hr.
First	2℃/min	750℃-25℃	-
Second	2℃/min	750℃-1000℃	2hrs
Third	3℃/min	1000℃-1350℃	2hrs
Fourth	5℃/min	1350- 30℃	17hrs

2.1 Physical test

2.1.1 Apparent density and porosity with water absorption

According to ASTM-C373, the physical testing is calculated by using these equations:

$$A \cdot P\% = ms - \frac{md}{ms} - mi \times 100\% \quad (1)$$

$$A.D = \left(\frac{md}{ms} - mi\right) \times \rho w \quad (2)$$

where,

md: Flint refractory mass when be dry (g);

mi: Flint refractory mass when be immersed (g);

ms: Flint refractory mass when be wet (g);

ρw: Water density (g/cm^3);

A.P: the apparent porosity (%);

A.D: the apparent density(g/cm^3).

2.1.2 Linear shrinkage test

Each of linear shrinkage and mass in Ignition was calculated according to ASTM-C1407 for Disc-shaped samples with a diameter of 25 mm, as in equations:

$$\text{L.S} = \frac{\text{Lo-L}}{\text{Lo}} \times 100\% \quad (3)$$

where,

Lo = Initial length before burning (mm);

L = Final length after burning (mm);

L.S = Linear shrinkage (unit less).

2.1.3 Analysis tests

X-ray diffraction (XRD) and scanning electron microscopy (SEM) analyses were conducted at the Nano Center of the University of Technology. The XRD measurements were performed using a Bruker diffractometer (Germany, 2010 model), while the SEM observations were carried out using an INSPECT S50 microscope (Holland). These techniques were employed to identify and characterize the various phases present in the flint-based refractory samples.

2.1.4 Thermal conductivity

The Lee's Disk Method, which is suitable for thermally insulating materials and samples with relatively low thickness compared to their diameter. The apparatus consists of a heater and three copper disks arranged in contact with the test specimen (*S*). The entire setup is enclosed in a glass chamber to minimize heat loss to the surroundings and to ensure measurement accuracy. Heating occurs by applying a controlled electrical voltage to the heater (6V), producing a steady current (0.25A) within the closed circuit. Heat is transferred directly to the adjacent copper disk and then conducted through the specimen to the lower disks until thermal equilibrium is achieved. The final steady-state temperatures of the disks (*A*, *B*, *C*) and the specimen (*S*) were recorded, along with the geometric parameters of the disks (diameter *r* and thickness *d*). The thermal conductivity coefficient (*k*) was calculated based on the measured heat flow rate using the following relation (in W/m·K):

$$\frac{K(T_B - T_A)}{ds} = e\left[T_A + \frac{2}{r\left(d_A + \frac{1}{4d_S}\right)T_S} + \frac{1}{2rd_ST_B}\right] \quad (4)$$

where,

V = applied voltage,

I = current,

A = cross-sectional area of the specimen,

d_s = sample thickness,

T_A= temperature for disc A,

T_B= temperature for disc B,

and $(T_B - T_A)$ = temperature difference between the upper and lower disks.

These parameters were determined under steady-state thermal conditions to ensure reliable and reproducible results.

3. RESULTS AND DISCUSSIONS

3.1 Physical properties

Pure Sample A (0% Bauxite + 10% Kaolin), Test results showed in Figures 3 and 4 that this Refractory had the highest apparent porosity (26%) compared to the other compositions, along with a low bulk density (2.08 g/cm³). These values are attributed to the absence alumina-rich addition that could induce the formation of dense crystalline phases such as mullite or corundum phases. XRD revealed the presence of limited crystalline phases, represented by cristobalite as in Figure 5 for pure flint and as in SEM Figure 6, along with the predominance of discontinuous glassy phase resulting from partial decomposition of kaolin and silica-rich flint. The presence of the discontinuous glassy phase causes pores to remain open, as silica melting under these conditions was insufficient to fill voids or seal the pores, contributing to increased porosity and water permeability. Studies indicate that the glassy phase produced by silica, in the absence of effective firing, leads to increased apparent porosity in refractory ceramics, as seen in Figures 3 and 4.

Adding (B) 10% coarse bauxite (particle size ≤ 1.18 mm) to the Refractory mixture (kaolin/flint) resulted in a significant decrease in apparent porosity from approximately 26% to approximately 17%, increase in bulk density from 2.08 g/cm³ to 2.25 g/cm³ as in Figures 3 and 4, This is attributed to the additional alumina contributing to the partial crystallization of the mullite phase during firing, which contributes to improved structural bonding and reduced open pores—a similar finding was found in the study [5] which showed that the addition of bauxite to flint reduced porosity and increased density due to alumina-based formation of mullite phase as in Figures 7 and 8 [5]. Similarly, the study examining the effect of alumina content on properties of mullite phase supports the hypothesis that increasing this alumina led to a decrease in porosity ratio by promoting a phase transition toward the mullite phase [6]. Furthermore, a review on the manufacture of mullite phase from extracted (kaolin and bauxite) is consistent with this interpretation, stating that the mullite phase acts as a major crystalline phase that reduces porosity and improves firing [7]. This is also confirmed by an Iraqi study that used alumina addition to a kaolin and bauxite mixture, finding that the associated high mullite phase content resulted in acceptable physical properties, with reduced porosity and increased density [8].

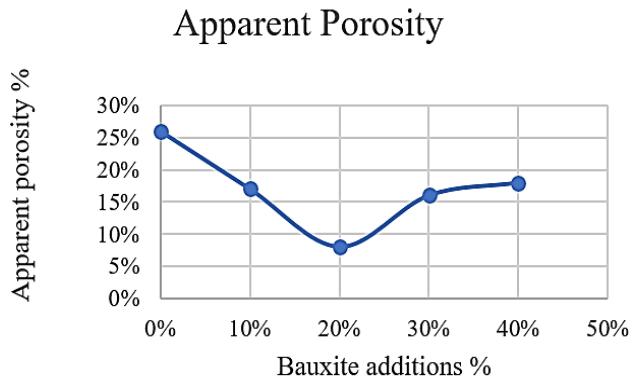

Figure 3. Apparent porosity for refractory flint-bauxite-10% kaolin

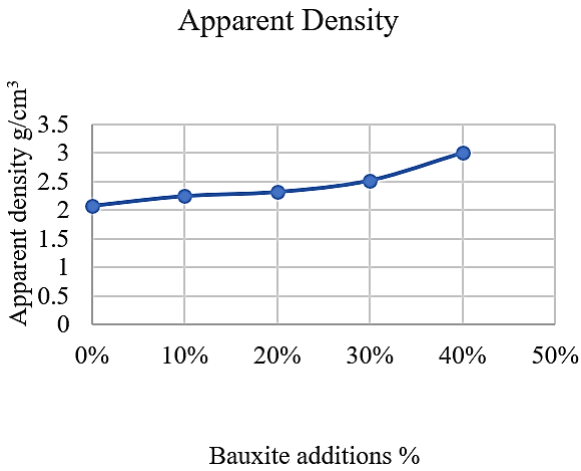

Figure 4. Bulk density for flint refractory flint-bauxite-10% kaolin

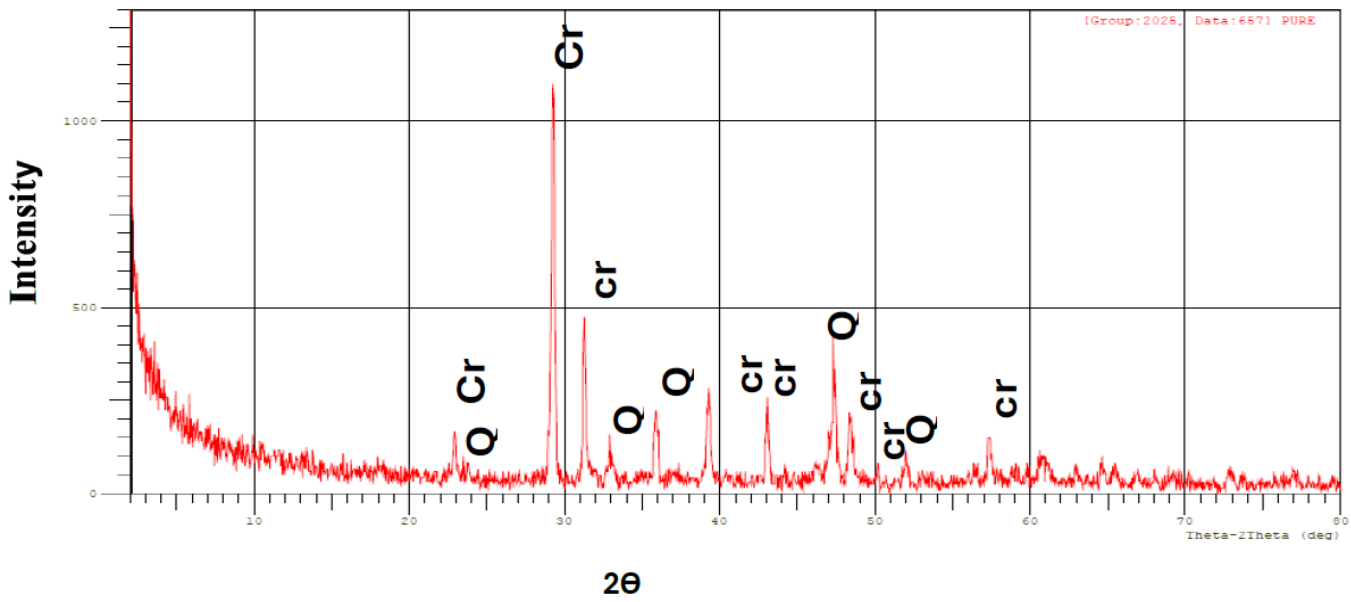

Figure 5. XRD for (A) pure refractory flint

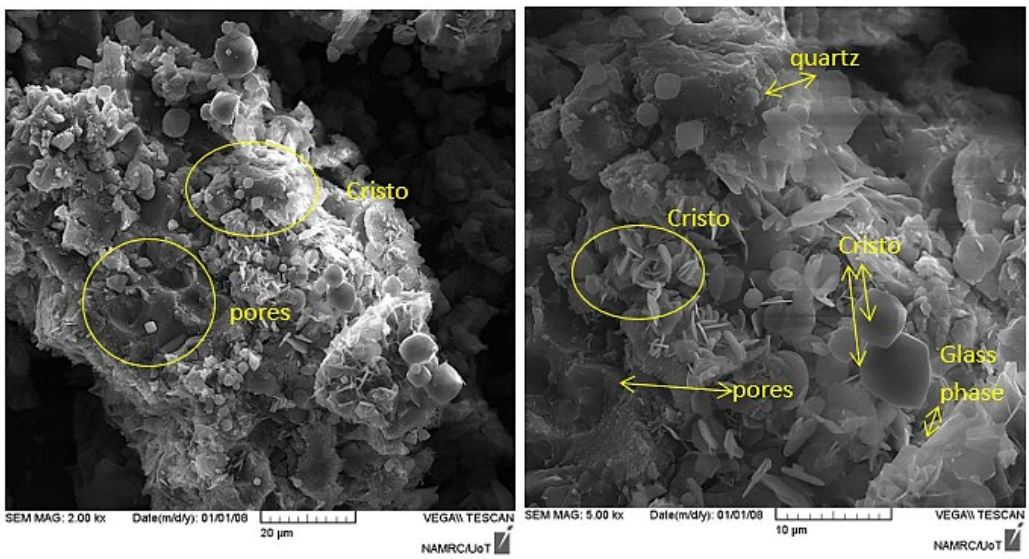

Figure 6. SEM for (A) pure flint refractory

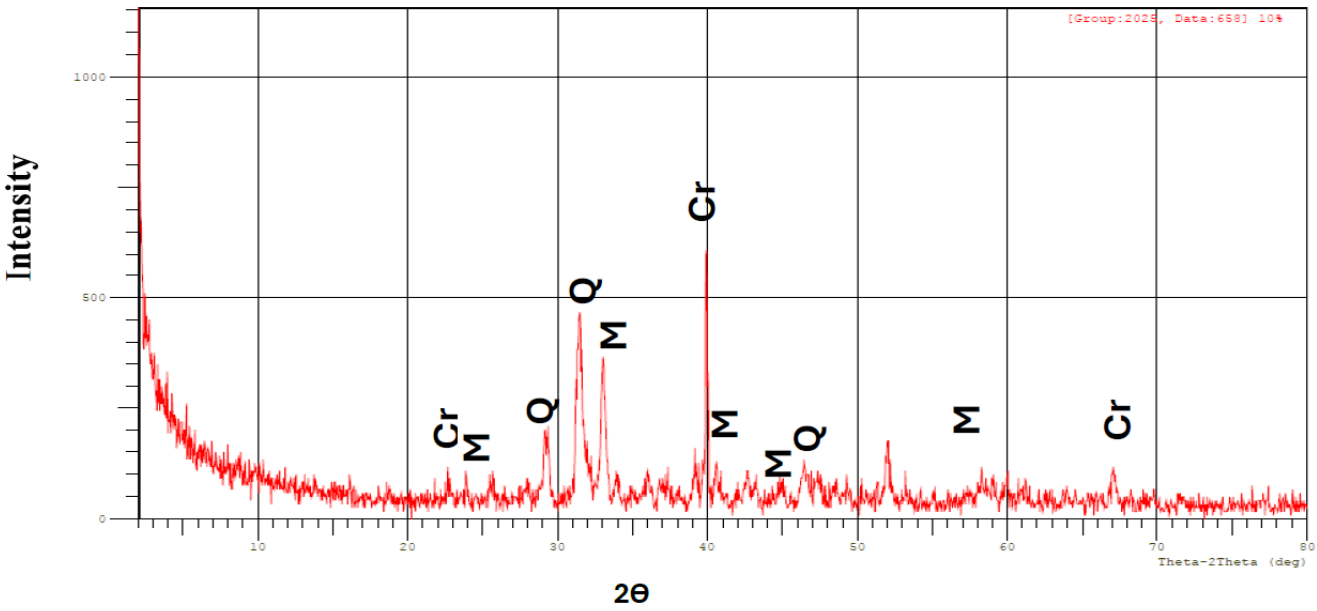

Figure 7. XRD for (B) refractory flint (10%) bauxite-10% kaolin

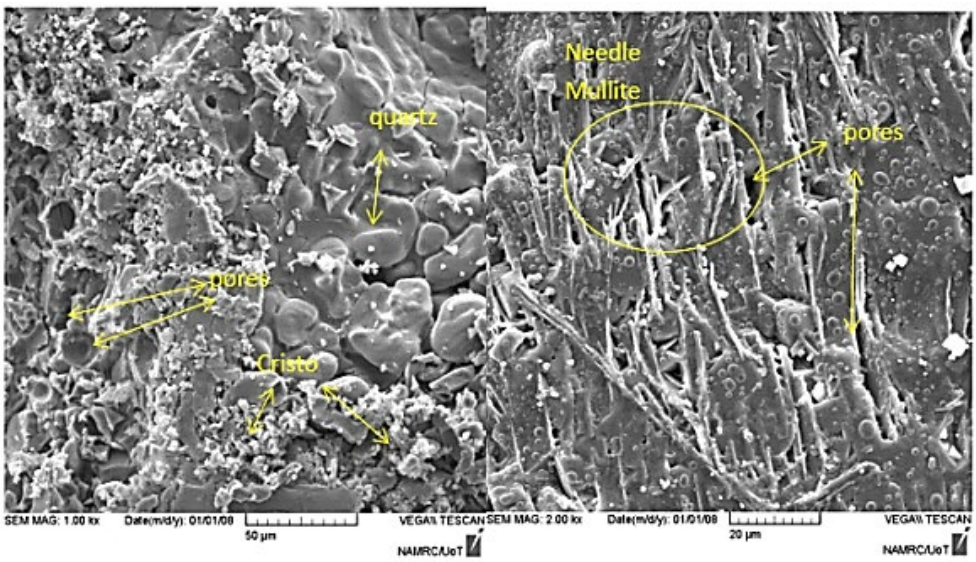

Figure 8. SEM for (B) refractory flint (10%) bauxite-10% kaolin

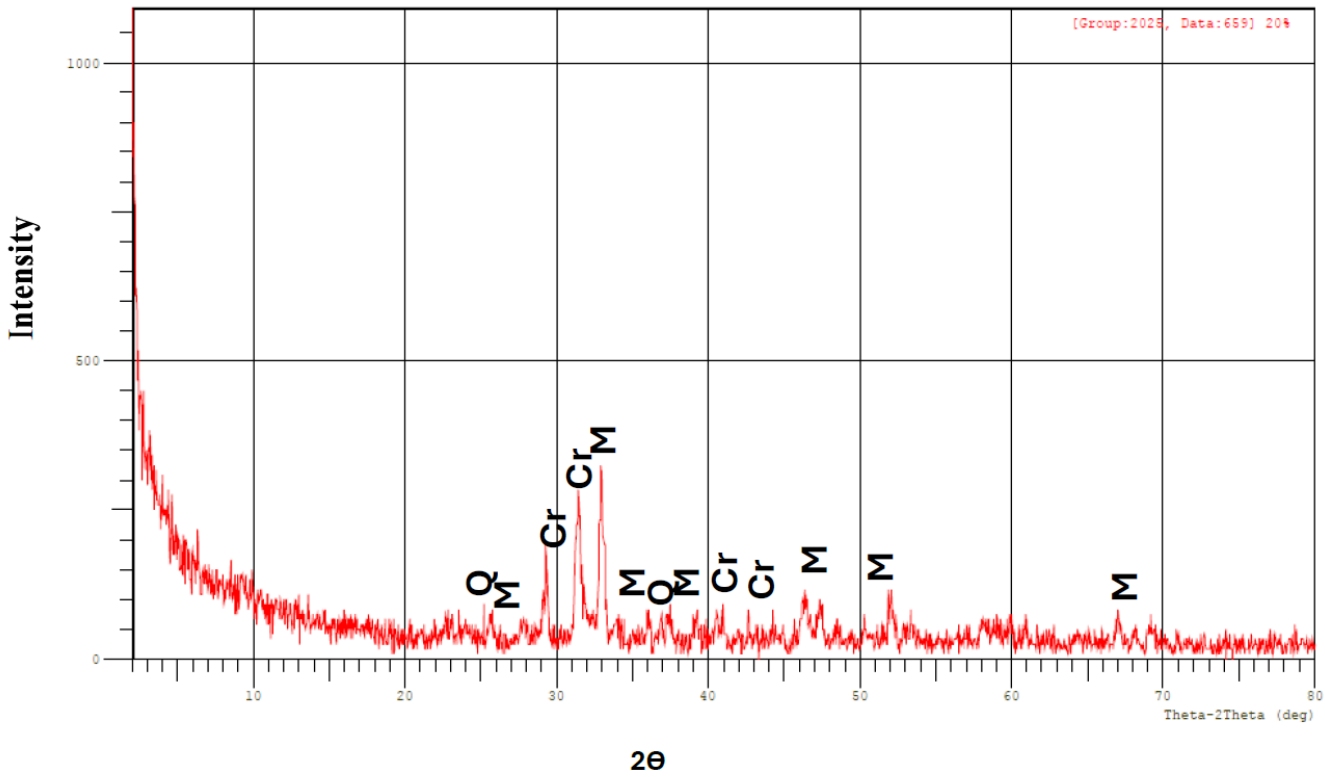

Figure 9. XRD for (C) refractory flint (20%) bauxite-10% kaolin

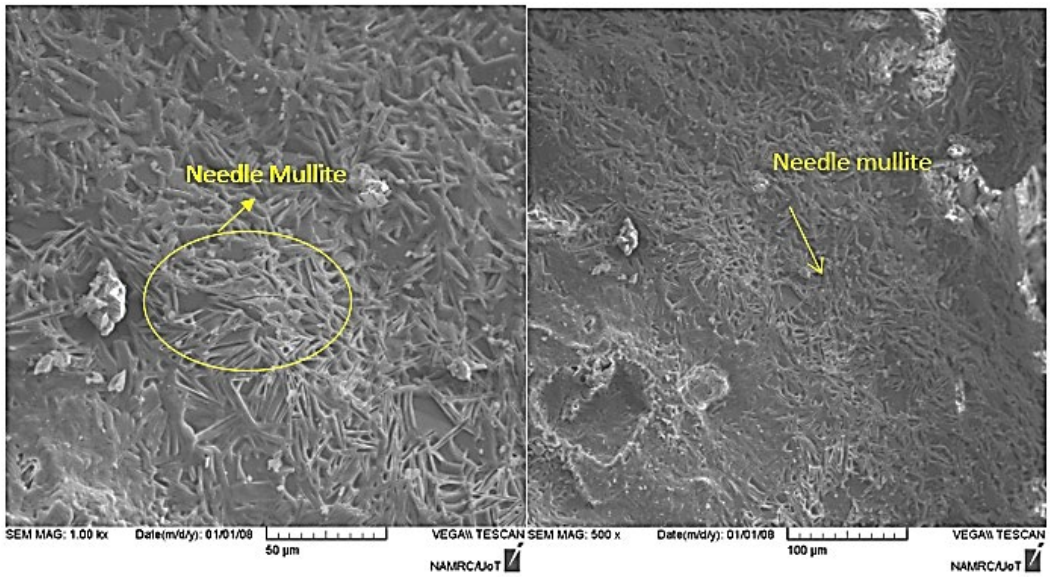

Figure 10. SEM for (C) refractory flint (20%) bauxite-10% kaolin

Refractory (C) (20% bauxite + 10% kaolin), This ratio represents the peak of firing in the system. Increasing the coarse bauxite content (particle size ≤ 1.18 mm) resulted in the formation of distinct mullite phase, with the presence of cristobalite phase. As in Figures 9 and 10. The consumption of large portion of the glassy phase in mullite phase formation resulted in pore shrinkage and increased structural compactness.

This was reflected in the physical properties, with apparent porosity decreasing from 17% to 8%, density increasing from 2.25g/cm³ to 2.32 g/cm³, the lowest value recorded among all compositions. This performance is attributed to effective firing supported by the residual liquid phase, and to the role of the needle mullite phase in promoting intergranular bonding and pore closure, which improved density and reduced permeability [9, 10].

This behavior is attributed to the optimal chemical balance between silica from flint and alumina introduced by bauxite, which approaches the stoichiometric ratio required for mullite formation ($3Al_2O_3 \cdot 2SiO_2$). At this composition, the reaction sintering process becomes highly efficient, producing fine, interlocking mullite crystals that fill intergranular voids and reduce the residual glassy phase. The liquid phase formed during sintering was sufficient to promote particle rearrangement and neck growth without causing exaggerated grain coarsening. Consequently, pore closure occurred more effectively, leading to a dense and uniform microstructure [10].

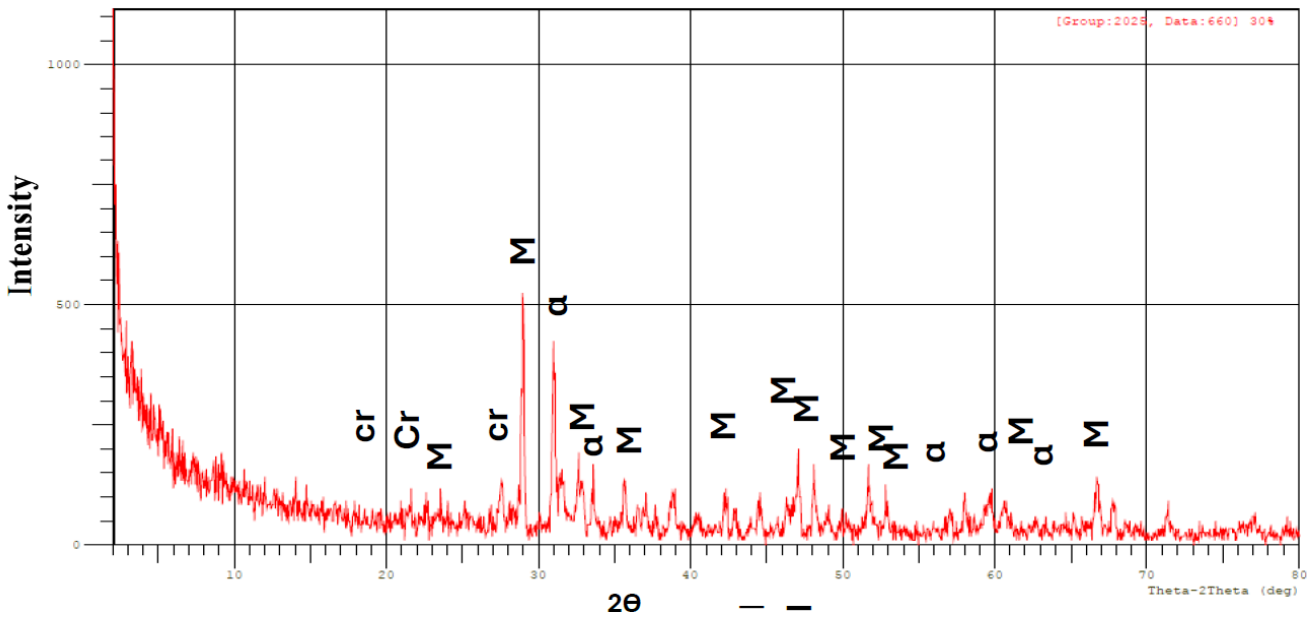

Figure 11. XRD for (D) for refractory flint 30%-bauxite-10% kaolin

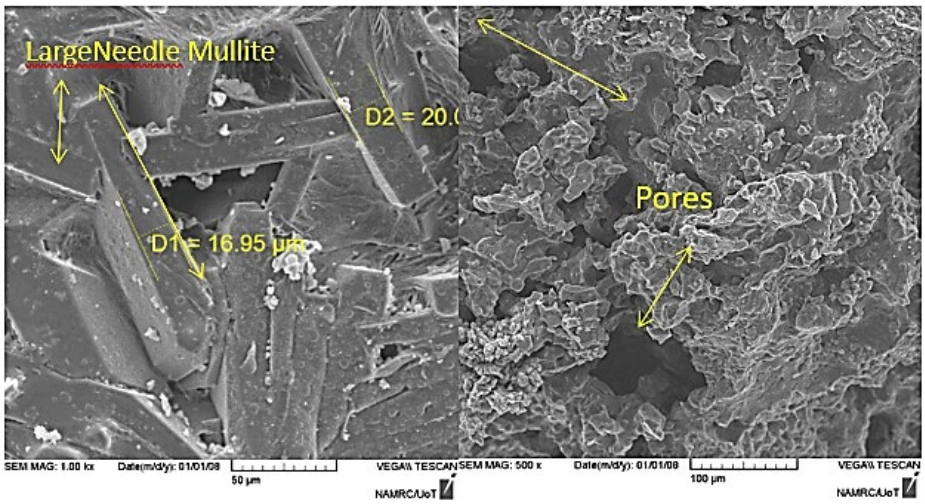

Figure 12. SEM for (D) for refractory flint 30%-bauxite-10% kaolin

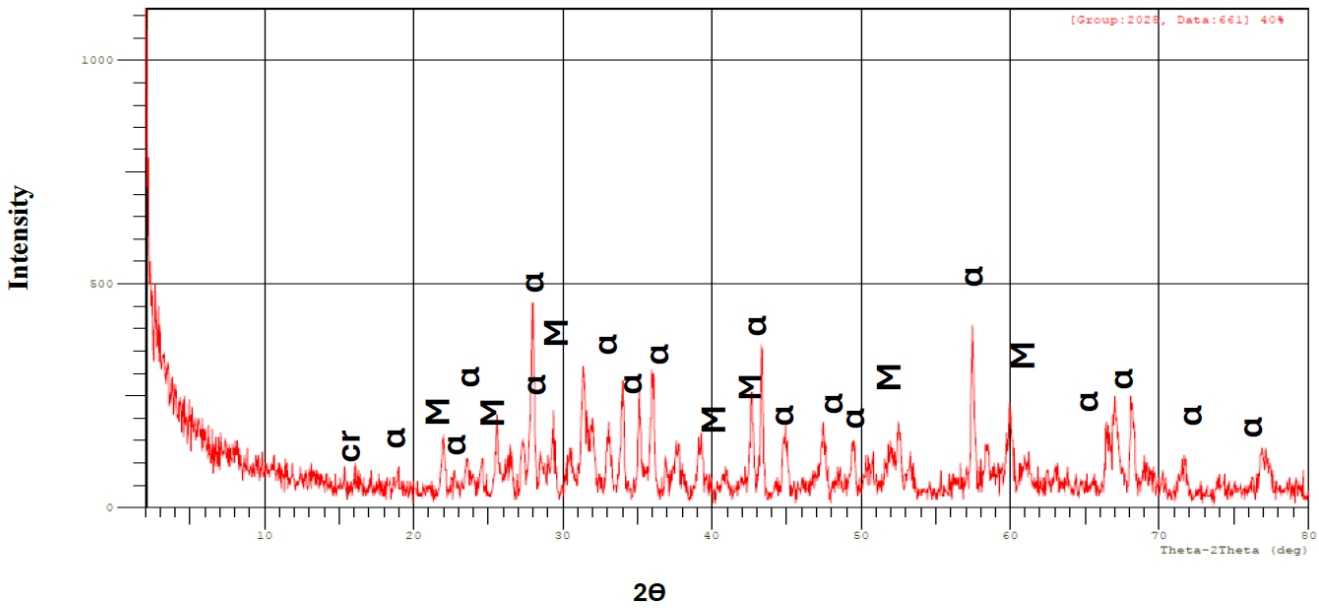

Figure 13. XRD-for (E) for refractory flint 40%-bauxite-10% kaolin

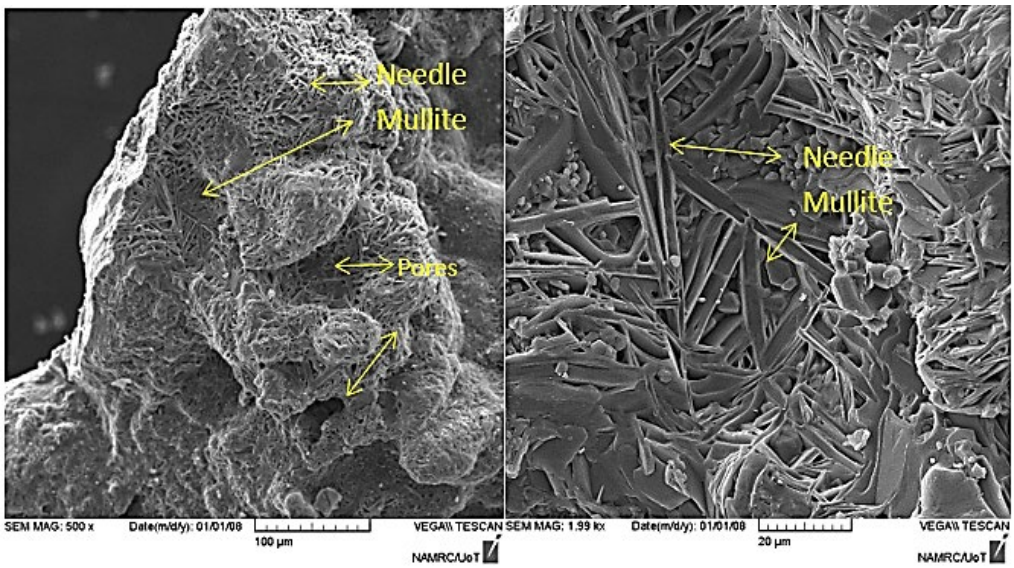

Figure 14. SEM for (E) for refractory flint 40%-bauxite-10% kaolin

Refractory (D, E) (30% - 40%bauxite + 10% kaolin), The increase in coarse bauxite enhanced the formation of mullite phase with the appearance of cristobalite phase and the highest proportion of mullite and corundum phases in 40 % among all samples (Figures 11-14). However, as in Figures 11 and 13 for XRD and as in Figures 12 and 14 for SEM, the porosity increased from 8% to 16% and reach to 18% due to the presence of a highly viscous glassy phase in small quantities and irregular distribution, in addition to gaps between large grains that were not fully closed due to poor local firing. Although the density increased from 2.32 g/cm³ to (2.52-reach to 3) g/cm³ due to the heavy phases (mullite, corundum, and bauxite) densities, the structure remained relatively open with 8% [11].

The evolution of porosity and bulk density in the present flint–bauxite–kaolin refractories can be strongly correlated with the effect of particle size on microstructural development. The high porosity is associated with the presence of a highly viscous residual glassy phase that did not effectively contribute to pore closure, The formation of non-densely packed acicular or needle mullite phase played a key role in raising the porosity level. It has been demonstrated that the use of coarse particles promotes the formation of larger mullite crystals that are poorly packed, leaving residual intergranular voids and consequently increasing the apparent porosity. This observation is consistent with [11], who reported that micronized additives in mullite–alumina ceramics prepared and led to coarser grain structures and higher open porosity compared to nanosized ones, due to incomplete packing and inefficient filling of the interstices [12, 13].

3.2 Linear shrinkage

The significant increase in the longitudinal shrinkage as appear in Figure 15 of the pure refractory (A) (7%) is attributed to the high amount of siliceous glassy phase resulting from the decomposition of kaolin and quartz-rich flint during firing. This phase is characterized by its high flowability under the influence of heat, which fills the interstitial spaces and promotes grain rearrangement, thus increasing the rate of longitudinal shrinkage. Studies have shown that the formation of glassy phases during firing acts as a liquid phase that facilitates thermal density and generates internal capillary pressure, leading to reduction in overall volume of ceramic structure [14].

The longitudinal shrinkage curve shows that adding (B)10% coarse bauxite to the flint–10% kaolin mixture did not significantly reduce shrinkage, with values remaining relatively high (6%) compared to the pure refractory. This is attributed to the solidification of the glassy phase; the surface tension forces pull the surrounding crystals and grains together. As this viscous phase cools and hardens, the contraction of the drawn particles results in a dimensional shrinkage of the ceramic body after firing. Furthermore, the moderate porosity (17%) allows the flow of the siliceous glassy phase and grain mobility, limiting the structure's ability to resist shrinkage [15, 16].

With the addition of 20% bauxite for sample(C), the acicular mullite phase begins to form clearly. This highly hard and thermally stable phase provides internal support that prevents grain realignment and limits longitudinal shrinkage, which drops to 5%. The higher density and lower porosity (8%) also reduce open pathways for structural shrinkage during firing. Furthermore, the lower glass phase content compared to 10% reduces the effect of viscous flow, enhancing shape stability during heat treatment [16].

When the bauxite content increases to 30–40% Refractory for (D, E), the linear shrinkage decreases to its lowest values (from 3% to 2.14%) compared to the rest of the Refractory. This is due to several interrelated factors, Increased formation of mullite and corundum phases, the high Al_2O_3 content at these ratios promotes the reaction between alumina and silica to production of mullite phase ($3Al_2O_3$ $2SiO_2$) in large quantities, with corundum (α-Al_2O_3) appearing, especially at 40%. These two phases are characterized by high density (3.16–3.98 g/cm³), excellent hardness, and thermal toughness, leading to the formation of a cohesive, interlocking crystal lattice that limits particle rearrangement during firing, thus reducing linear shrinkage rates [17, 18].

Decrease in the glass phase, at these ratios, most of the silica is consumed in the production of mullite rather than the formation of the glass phase. Since the glassy phase is responsible for the viscous flow that facilitates shrinkage, its decrease reduces the structure's ability to shrink under heat, explaining the low linear shrinkage values. Also, Effect of the Coarse Grain Size of Bauxite, the introduction of coarse

bauxite grains creates the occurrence of crystal growth leads to the formation of large crystals of mullite phase, which in turn hinder dense packing micro-voids between the larger grains, and these micro-voids do not shrink linearly during firing. This mechanical effect reduces overall shrinkage despite the high bulk density, as some micro-voids remain incompletely incorporated within the matrix. The balance between Density and Porosity, Although the overall density increases at these ratios (3 g/cm³ at 40%), the presence of micro-voids resulting from the coarse grains prevents excessive shrinkage, providing better dimensional stability compared to lower bauxite ratios [19, 20].

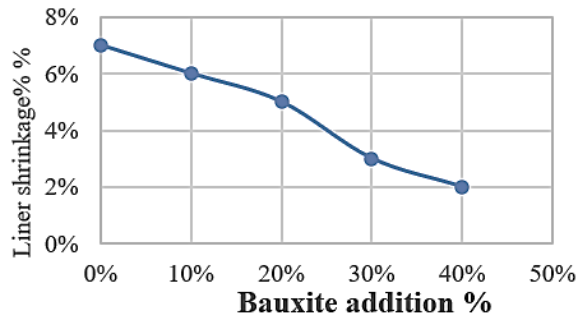

Figure 15. Linear shrinkage for flint-bauxite-10% kaolin refractory

3.3 Thermal conductivity

Measurement results showed, as shown in Figure 16, that the pure refractory (A), composed of flint with 10% kaolin, showed improved thermal conductivity compared to the 30%-40% refractory. This behavior is attributed to the abundance of the glassy phase formed by the reaction between flint and kaolin during firing. The glassy phase provides a relatively continuous network, which facilitates semi-continuous pathways for heat transfer. Although this pure refractory retained a relatively high level of porosity, the dominant effect of the glassy phase counteracted the negative influence of the pores and contributed to a notable increase in thermal conductivity [21].

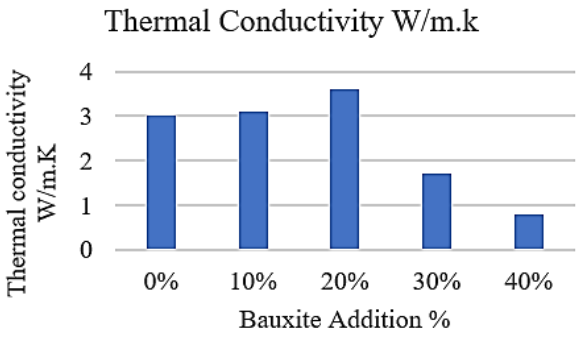

Figure 16. Thermal conductivity results for flint bauxite-10% kaolin refractory

At 10% bauxite addition for (B), a marked reduction in porosity was observed, accompanied by the initial formation of mullite phase within the refractory matrix. This microstructural development enhanced grain-to-grain bonding and increased the fraction of stable crystalline phases relative to the glassy phase, thereby establishing more efficient solid pathways for heat transfer and improving the thermal conductivity. At 20% bauxite for (C), the porosity reached its minimum value (8%) in parallel with the distinct appearance of mullite phase as a dominant crystalline phase. The combined effect of reduced porosity and a higher content of thermally stable crystalline phases provided a dense and well-connected network, which facilitated heat transport and resulted in the highest thermal conductivity among all studied compositions [21].

At 30%-40% bauxite addition for (D, E), the porosity increased again as a result of the coarse particle size creates the occurrence of crystal growth, leading to the formation of large crystals of mullite phase, which in turn hinders dense packing, which limits the closure of intergranular voids during firing. Although mullite phase formation continued to develop within the structure, the influence of the open and interconnected porosity became the dominant factor, restricting the continuity of solid conduction paths and leading to noticeable reduction in thermal conductivity. Also, the unfilled pores generated by the excessive coarseness of the aggregates and the incomplete densification process [22]. The elevated porosity at this stage dominated the positive contribution of mullite phase and corundum phase, thereby intensifying phonon scattering and hindering heat transfer, which resulted in the lowest thermal conductivity among all investigated samples [23]. The thermal conductivity behavior of the studied flint-bauxite-10% kaolin refractories can be directly explained by the presence of coarse bauxite grains and the subsequent formation of coarse mullite phase. When coarse particles dominate, the resulting mullite tends to crystallize in larger, less interlocked morphologies, leaving intergranular pores and discontinuities in the solid network [24]. These voids interrupt phonon transport and reduce the efficiency of heat conduction, thereby lowering the overall thermal conductivity despite the intrinsic conductivity of mullite and corundum phases [25-27]. Similarly demonstrated that the incorporation of microsized additives in mullite–alumina ceramics produced coarser grain structures with higher porosity, which disrupted thermal transport pathways compared to ceramics reinforced with nanosized particles. This confirms that the coarse particle size not only governs porosity but also directly dictates the thermal conduction response of the refractory body.

4. CONCLUSIONS

Iraqi flint was strengthened by integrating locally sourced kaolin with very coarse-grained Iraqi bauxite, which stimulated the formation of coarse loosely packed mullite phase by deliberate enlargement of the coarse fraction in flint–bauxite–kaolin refractories simultaneously increased bulk density and porosity while minimizing linear shrinkage. This atypical combination establishes the present work as a contribution that redefines the role of the coarse fraction as a design variable rather than a limitation.

Pure Refractory (Flint + 10% Kaolin): High porosity (26%), low density (2.08 g/cm^3), and high shrinkage due to glassy phase and poor firing.

10% Bauxite: Porosity decreased (17.2%), density increased (2.25 g/cm³), with initial mullite phase formation and moderate firing improvement.

20% Bauxite: Lowest porosity (8.15%), density 2.32 g/cm^3, significant mullite phase growth and pore closure led to best

structural cohesion.

30% Bauxite and 40% Bauxite: Porosity rise again (16%) despite higher density (2.52 g/cm^3) at 30%; Porosity 18.18% with highest density (3.00 g/cm^3) at 40%, coarse grains created interpore due to occurrence of crystal growth leads to formed a large crystal of mullite phase which in turn hinder dense packing, so reducing shrinkage with leaving open porosity.

The 20% coarse bauxite addition provides the optimal balance of low porosity, high density, and improved firing, making it the most suitable formulation for refractory bricks.

Thermal conductivity improved markedly up to 30% bauxite, driven by the crystallization of mullite and corundum that facilitated heat transport through a denser phase network.

At 40% bauxite, conductivity declined due to the dominance of open porosity associated with loosely packed mullite crystals, which disrupted continuous heat pathways.

Finally, the formation of non-dense mullite from coarse bauxite is a distinctive advantage, as it not only enhanced thermal shock resistance but also provided a pathway to upgrade Iraqi flint refractories into more competitive high-temperature materials.

This indicates that balancing the growth of crystalline phases while maintaining adequate porosity is effective strategy for improving the thermal performance of refractories in high-temperature applications.

REFERENCES

[1] Jabbar, H., Muhi, E., Hussien, T. (2023). Preparing and investigating the structural properties of porous ceramic nano-ferrite composites. Journal of Applied Sciences and Nanotechnology, 3: 34-41. https://doi.org/10.53293/jasn.2022.4804.1150

[2] Gata, F.H., Mhui, E. (2022). Study of the mechanical and thermal properties of refractory mortars from kaolin and bentonite. Journal of Applied Sciences and Nanotechnology, 2(1): 69-79. https://doi.org/10.53293/jasn.2021.3743.1039

[3] Hadi, E.M. (2017). Manufacturing of refractory bricks from Iraqi flint. Journal of Engineering and Technology, 35(1): 161-171.

[4] Sadik, C., El Amrani, I.E., Albizane, A. (2014). Recent advances in silica-alumina refractory: A review. Journal of Asian Ceramic Societies, 2(2): 83-96. https://doi.org/10.1016/j.jascer.2014.03.001

[5] H. Al-Taie, M., H. Ali, A., F. Al-Attar, A. (2014). Characterizations of semi-silica refractory bricks produced from local Iraqi materials. Engineering and Technology Journal, 32(9): 2268-2276. https://doi.org/10.30684/etj.32.9A13

[6] Jasim, S.L., Aaidan, S.A., Hadi, E.M. (2024). Refractory mullite phase enhancement in silicon carbide/kaolin composites. Journal of Applied Sciences and Nanotechnology, 4(3): 42-52. https://doi.org/10.53293/jasn.2024.7257.1271

[7] Liu, J., Li, Y., Li, S., Xu, N., Xiang, R., Wang, Q. (2019). Micro-porosity and properties of light-weight insulation refractories based on calcined flint clay. Transactions of the Indian Ceramic Society, 78(1): 7-12. https://doi.org/10.1080/0371750X.2019.1566023

[8] Omar, M.H., Zaidan, S.A. (2017). Preparation of refractory mortars from kaolin with bauxite and flint additives. International Journal of Innovative Research in Science, Engineering and Technology, 6(5): 8693-8698.

[9] Abdul-Hamead, A.A. (2011). Studying the effect of adding Doekhla kaolin clay and alumina to Iraqi bauxite on some physical, mechanical, and thermal properties. Al-Khwarizmi Engineering Journal, 7(1): 95-105. https://www.alkej.uobaghdad.edu.iq/index.php/alkej/article/view/473.

[10] Liu, Z., Lian, W., Liu, Y., Zhu, J., Xue, C., Yang, Z., Lin, X. (2021). Phase formation, microstructure development, and mechanical properties of kaolin-based mullite ceramics added with Fe2O3. International Journal of Applied Ceramic Technology, 18(3): 1074-1081. https://doi.org/10.1111/ijac.13720

[11] Mahnicka-Goremikina, L., Rundans, M., Goremikins, V., Svinka, R., Svinka, V., Orlova, L., Juhnevica, I. (2024). Effect of microsize and nanosize TiO2 on porous mullite-alumina ceramic prepared by slip casting. Materials, 17(24): 6171. https://doi.org/10.3390/ma17246171

[12] Lima, L.K.S., Silva, K.R., Menezes, R.R., Santana, L.N.L., Lira, H.L. (2022). Microstructural characteristics, properties, synthesis and applications of mullite: A review. Cerâmica, 68(385): 126-142. https://doi.org/10.1590/0366-69132022683853184

[13] Yuan, L., Liu, Z., Yan, Z., Jin, E., Tian, C., Yu, J. (2022). Effect of mullite phase formed in situ on pore structure and properties of high-purity mullite fibrous ceramics. Ceramics International, 48(3): 3578-3584. https://doi.org/10.1016/j.ceramint.2021.10.136

[14] Raut, N.S., Biswas, P., Bhattacharya, T.K., Das, K. (2008). Effect of bauxite addition on densification and mullitization behaviour of West Bengal clay. Bulletin of Materials Science, 31(7): 995-999. https://doi.org/10.1007/s12034-008-0156-4

[15] Silva, L.B.D., Blaese, D., Peres, A.P.D.S., Costa, A.C.S.D., Acchar, W. (2020). Effect of the addition of glasses as sintering aids on microstructure and properties of nanoalumina. Matéria (Rio de Janeiro), 25(1): e-12584. https://doi.org/10.1590/S1517-707620200001.0910

[16] Chen, C.Y., Lan, G.S., Tuan, W.H. (2000). Preparation of mullite by the reaction sintering of kaolinite and alumina. Journal of the European Ceramic Society, 20(14-15): 2519-2525. https://doi.org/10.1016/S0955-2219(00)00125-4

[17] Assy, N.A., Hadi, E.M. (2025). Study of the mechanical and microstructure properties of zirconia reinforced with glass and silica. International Journal of Nanoelectronics and Materials, 18: 1-8. https://doi.org/10.58915/ijneam.v18ijune.2302

[18] Hadi, E.M., Abdul-Hussien, H.J. (2019). Preparation of ceramic foam from porcelanite by using simple direct foaming method. AIP Conference Proceedings, 2123(1): 020007. https://doi.org/10.1063/1.5116934

[19] Zawrah, M.F.M., Khalil, N.M. (2001). Effect of mullite formation on properties of refractory castables. Ceramics International, 27(6): 689-694. https://doi.org/10.1016/S0272-8842(01)00021-9

[20] Zemánek, D., Lang, K., Tvrdík, L., Všianský, D., et al. (2021). Development and properties of new mullite based refractory grog. Materials, 14(4): 779. https://doi.org/10.3390/ma14040779

[21] Zheng, W., Wu, J.M., Chen, S., Wang, C.S., et al. (2021). Influence of Al2O3 content on mechanical properties of

silica-based ceramic cores prepared by stereolithography. Journal of Advanced Ceramics, 10(6): 1381-1388. https://doi.org/10.1007/s40145-021-0513-y

[22] Richet, P., Bottinga, Y., Danielou, L., Petitet, J.P., Tequi, C. (1982). Thermodynamic properties of quartz, cristobalite and amorphous SiO2: Drop calorimetry measurements between 1000 and 1800 K and a review from 0 to 2000 K. Geochimica et Cosmochimica Acta, 46(12): 2639-2658. https://doi.org/10.1016/0016-7037(82)90383-0

[23] Stabler, C., Reitz, A., Stein, P., Albert, B., Riedel, R., Ionescu, E. (2018). Thermal properties of SiOC glasses and glass ceramics at elevated temperatures. Materials, 11(2): 279. https://doi.org/10.3390/ma11020279

[24] Schneider, H., Fischer, R.X., Schreuer, J. (2015). Mullite: Crystal structure and related properties. Journal of the American Ceramic Society, 98(10): 2948-2967. https://doi.org/10.1111/jace.13817

[25] Kingery, W.D., Bowen, H.K., Uhlmann, D.R., Frieser, R. (1977). Introduction to ceramics. IOP Science, 124: 3. https://doi.org/10.1149/1.2133296

[26] Chen, F., Sang, S., Ma, Y., Li, Y. (2024). Preparation of microporous mullite refractories with high strength based on low-grade bauxite and coal gangue. International Journal of Applied Ceramic Technology, 21(3): 1648-1657. https://doi.org/10.1111/ijac.14626

[27] Al-Amer, E.M.H., Al-Kadhemy, M.F.H. (2015). Improving the physical properties of Iraqi bauxite refractory bricks. Al-Nahrain Journal of Science, 18(3): 67-73. https://mail.anjs.edu.iq/index.php/anjs/article/view/312/254.